Applied Surface Science 605 (2022) 154615

Contents lists available at ScienceDirect

Applied Surface Science

journal homepage: www.elsevier.com/locate/apsusc

Deep investigation of two-dimensional structure arrays formed on Si surface

Ruiyan Li [a,b], Xiuyun Li [a,b], Tingting Zou [a,b], Wufeng Fu [a,b], Jun Xing [d], Tao Huang [a,b], Zhi Yu [a,b,c,*], Jianjun Yang [a,b,*]

[a] GPL Photonics Laboratory, State Key Laboratory for Applied Optics, Changchun Institute of Optics, Fine Mechanics and Physics, Chinese Academy of Sciences, Changchun 130033, China
[b] University of Chinese Academy of Sciences, Beijing 100049, China
[c] The Key Laboratory of Bionic Engineering (Ministry of Education), Jilin University, Changchun 130012, China
[d] Xinjiang Key Laboratory of Solid State Physics and Devices, School of Physics and Technology, Xinjiang University, 666 Shengli Road, Urumqi 830046, China

ARTICLE INFO

Keywords:
Femtosecond laser
2D periodic structure arrays
Dynamic interference positive feedback
Self-regulatory SPP excitation

ABSTRACT

Femtosecond laser-induced micro and nanostructures have been widely explored, because of their exhibiting great potential applications in many areas. However, the flexible control of the surface structure in both morphology and arrangement regularity still needs further investigation. This paper presents a maskless method to fabricate the two-dimensional periodic arrays of nanostructures on silicon surface based on the surface wave self-regulatory effect upon irradiation of the circularly polarized femtosecond laser. The spatial period of the regular structure arrays exhibit the alterable and constant values in the directions parallel and perpendicular to the sample scanning, respectively, the latter of which is highly dependent on the laser scanning speed. The formation mechanisms of the periodic structure arrays are explored through simulations with both the finite-difference time-domain method and the dynamic interference positive feedback model. The dynamic modulation of the laser energy on Si surface is revealed to originate from the self-regulatory effect during the laser processing. In addition, the depth of the two-dimensional structure arrays can be further experimentally adjusted from 74.5 nm to 112 nm by HF etching process.

1. Introduction

Over the past decades, the generation of periodic micro and nanostructures has been extensively studied by researchers because of its well-known advantages for the light manipulation in the amplitude [1], phase [2], polarization [3], and frequency [4], which provides numerous important application prospects [5–7]. Up to now, although some mature technologies including electron beam lithography [8], focused ion beam milling [9], and photolithography [10], have been widely used for the high resolution manufacturing, they are still limited by the intrinsic shortcomings, such as the costly equipment, complex procedures, and masking requirement. With the rapid development of femtosecond laser, it has been proved as a new powerful and versatile tool for the high precision manufacture based on the unique properties of the high efficient and convenient production without non-material selection, which has been already successfully employed in many areas, such as the medical treatment, nanophotonics, bio-sensors, micro or nanofluid [11–13].

As a universal phenomenon of the femtosecond laser-material interaction especially with the energy fluence close to the damage threshold, the laser-induced periodic surface structure (LIPSS) was found to possess capabilities of easily gaining the subwavelength or even deep-subwavelength fabrication on a variety of materials. In spite of dispute, the underlying formation mechanisms have been largely attributed to interference of the incident laser with the excited surface plasmon polaritons (SPPs) or the scattered waves, leading to the spatially periodic distribution of the laser energies on the material surface [14–17]. In the previous studies, one-dimensional (1D) grating-like LIPSS has been successfully implemented on different materials [18,19]. Although they were mostly performed with the linear polarization of the incident laser pulses [18,19], both the control of the SPP excitation and the structure arrangements are still restricted [14,15,20,21]. To

* Corresponding authors at: GPL Photonics Laboratory, State Key Laboratory for Applied Optics, Changchun Institute of Optics, Fine Mechanics and Physics, Chinese Academy of Sciences, Changchun, China.
E-mail addresses: zyu@imr.ac.cn (Z. Yu), jjyang@ciomp.ac.cn (J. Yang).

https://doi.org/10.1016/j.apsusc.2022.154615
Received 11 May 2022; Received in revised form 9 August 2022; Accepted 17 August 2022
Available online 1 September 2022

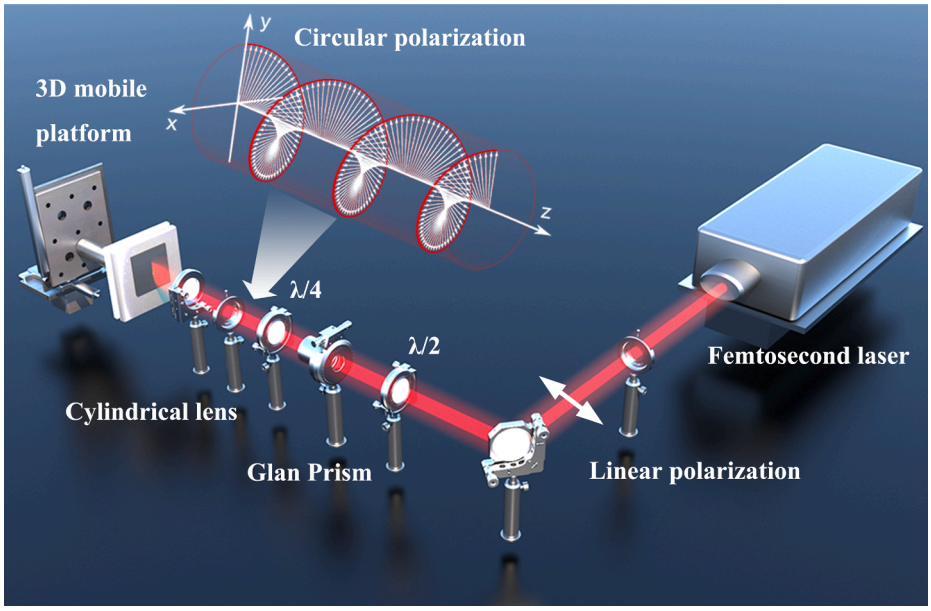

Fig. 1. Schematic diagram of the experimental setup for the femtosecond laser fabrication.

surmount the barrier of the traditional 1D LIPSS formation, our research group previously reported a method of producing two-dimensional (2D) periodic subwavelength structure arrays under irradiation of the picosecond time-delayed double femtosecond laser pulses on metal surfaces [22,23]. In addition, through using the circular polarization of femtosecond lasers, other authors have also demonstrated the generation of 2D surface structures [24,25], however, their using spherical focal lens make the high regular structure formation become often hard [26–28].

Herein, we proposed a high-efficient controllable method for fabricating the 2D structure arrays by the cylindrical focusing of the femtosecond laser on Si surface. It is revealed that the surface morphology induced by the antecedent laser pulse irradiation tends to modulate the SPP excitation of the follow-up laser pulse irradiation, and the consequent re-distribution of the laser intensity can further affect the structure development, which constitutes positive feedbacks via the mutual interaction between the laser and surface structures. Through observing the evolution of surface morphology with different numbers of laser pulse irradiation, we can divide the formation of 2D periodic nanostructures into three processes, which are further verified by the simulations of both the finite-difference time-domain (FDTD) method and the dynamic interference positive feedback (DIPF) model. In addition, the structure period in the scanning direction can be tuned by varying the scanning speed.

2. Experimental

2.1. Femtosecond laser processing scheme and characterization

A schematic of the experimental setup is demonstrated in Fig. 1, where the laser source is a commercially available chirped pulse amplification of Ti sapphire femtosecond laser (Spectra-Physics HP-Spitfire 50) system, to deliver the pulse trains at the repetition rate of 1 kHz with the central wavelength of 800 nm and the time duration of 40 fs. A cylindrical lens (f = 50 mm) was employed to focus the femtosecond laser beam on the polished Si wafers (1 0 0) in ambient air. The incident laser energy was controlled by the combination of a Glan prism and a half-wave plate. A quarter wave-plate (zero-order) was used for transforming the femtosecond laser from the linear polarization into the elliptical or circular state. The spatial length and width of the focused laser beam spot were estimated about 5 mm and 10.3 μm, respectively, via Zemax software, as shown in Fig. S1. A three dimensional translating stage was adopted to fix the sample and have a precisely controllable movements. An electrical shutter (SH05) was inserted into the optical path to control the number of laser pulse accumulation on the sample surface. The morphologies of the laser-induced surface structures were characterized by both a scanning electron microscope (SEM, Hitachi S-4800) and an atomic force microscope (AFM, Bruker).

2.2. Theoretical simulations

The electric (E)-field distribution of the laser intensity on the sample surface during the femtosecond laser processing was simulated with the FDTD method (Lumerical software package). The simulation details are clearly shown by a diagram in Fig. S2. During the whole simulation, we employed two different surface conditions: the initially laser-damaged random morphology and the regular structure arrangement. Accordingly, the idea of this simulation is to quantitatively reveal that the incident laser field distribution can be spatially modulated by the surface structures. In other words, the generation of the stable laser field distribution is very physically required for the following periodic structure formation. In contrast, the DIPF simulation was carried out with MATLAB (R2014 b) software (see the supporting information B for details). It is actually based on the SPP interference to present the dynamic process of the surface wave self-regulating, which can reveal the positive feedback modulations between the surface morphology and the SPP excitation during the laser processing. The entire evolution process includes multiple calculation iterations with the continuous irradiation of laser pulses, each of which only concentrates on a process of how one laser pulse is modulated in the field intensity via the particular surface morphology. Both the FDTD and DIPF simulations have their own unique features for the understanding of LIPSS development. The former method can clearly demonstrate the influence of the experimentally measured surface morphology on the field intensity distribution of the following laser pulse irradiation, but it cannot show the dynamic evolution process. That is, it only concerns the issue at one specific temporal stage of LIPSS growth. Whereas, the DIPF simulation can present the dynamic physical pictures during the LIPSS formation, in which the employed surface morphologies at the intermediate stages cannot be observed. Anyway, the purpose of our using the two simulations tries to provide deep insights into the whole LIPSS formation, especially when their different description aspects are mutually complemented each

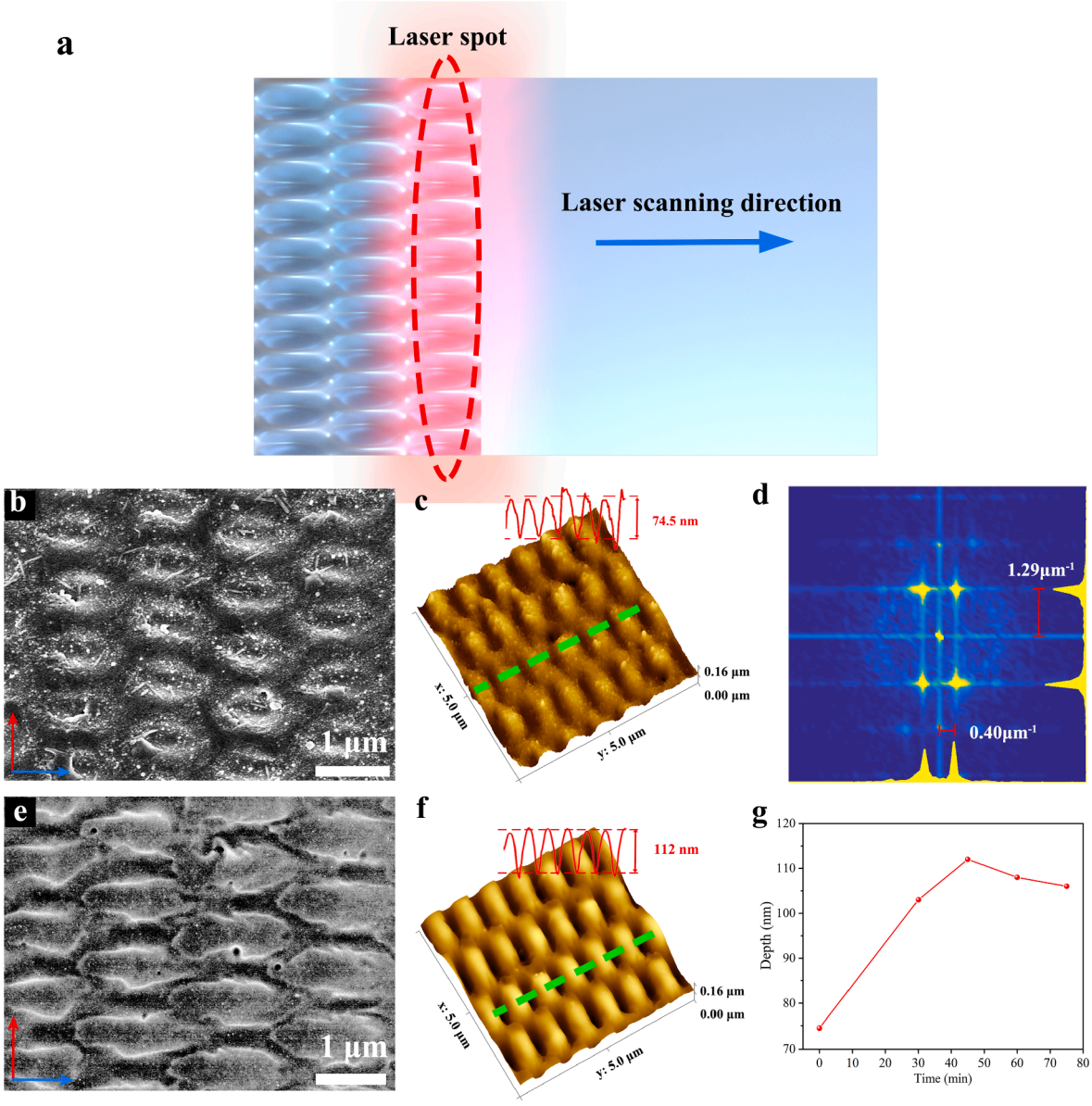

Fig. 2. (a) Schematic diagram of the laser scanning. (b) SEM image of the two-dimensional structure arrays on Si wafer (1 0 0) produced by the femtosecond laser with the scanning speed of V = 1.2 mm/s and the laser fluence of F = 245.65 mJ/cm^2. (c) AFM and (d) 2D-FFT analysis of the two-dimensional structure arrays on Si surface. (e) SEM image and (f) AFM morphology of the 2D periodic structure arrays after etching in 5 % HF for 45 min. (g) The measured variation of the structure depth as a function of etching time. The scale bar is 1 μm. The red and blue arrows are directions perpendicular and parallel to the scanning, respectively.

other, i.e, the finally observed regular structures are originated from the positive feedback self-regulating processes between the surface morphology and the surface wave excitation.

3. Results and discussion

3.1. Femtosecond laser patterning of 2D structure arrays on Si surfaces

During the experiment, the laser-induced surface structures were firstly carried out by the sample scanning with a speed of V = 1.2 mm/s at the incident laser fluence of F = 245.65 mJ/cm^2. After that, the laser-exposed sample was ultrasonically cleaned in deionized water and ethanol for 20 min and then followed by the blow-drying with N_2. Fig. 2a shows a relationship between the laser scanning process and the 2D periodic arrays structure formation. As shown in Fig. 2b, 2D periodic arrays of the spindle-like nanostructures are presented on Si surface, with a column spacing of each period of Λ = 1.2 μm and a period of Λ = 775 nm in the directions parallel and perpendicular to the scanning direction (denoted by the blue single-head arrow), respectively. Their corresponding cross-section images are illustrated in Fig. S3. The AFM measurement of the structure depth approximated 74.5 nm (Fig. 2c). The corresponding fast Fourier transform (FFT) image of the surface structures is shown in Fig. 2d, where the distinct distribution of the bright dots indicates the high regular profile of the structures in the spatial domain. In terms of the FFT spectra, the measured frequency spacing has a value of 0.4 μm^{-1} and 1.29 μm^{-1} in the directions parallel and perpendicular to the sample scanning, respectively.

According to the previous study [29], the interaction between the femtosecond laser and the semiconductor surface often undergoes the following physical stages: (i) the carrier excitation, (ii) the carrier thermalization, (iii) the carrier recombination, and (iv) the thermal and structuring effects. The final stage can be presented by melting, evaporation, thermal diffusion and re-solidification. As for the material of silicon, the femtosecond laser processing starts with the generation of

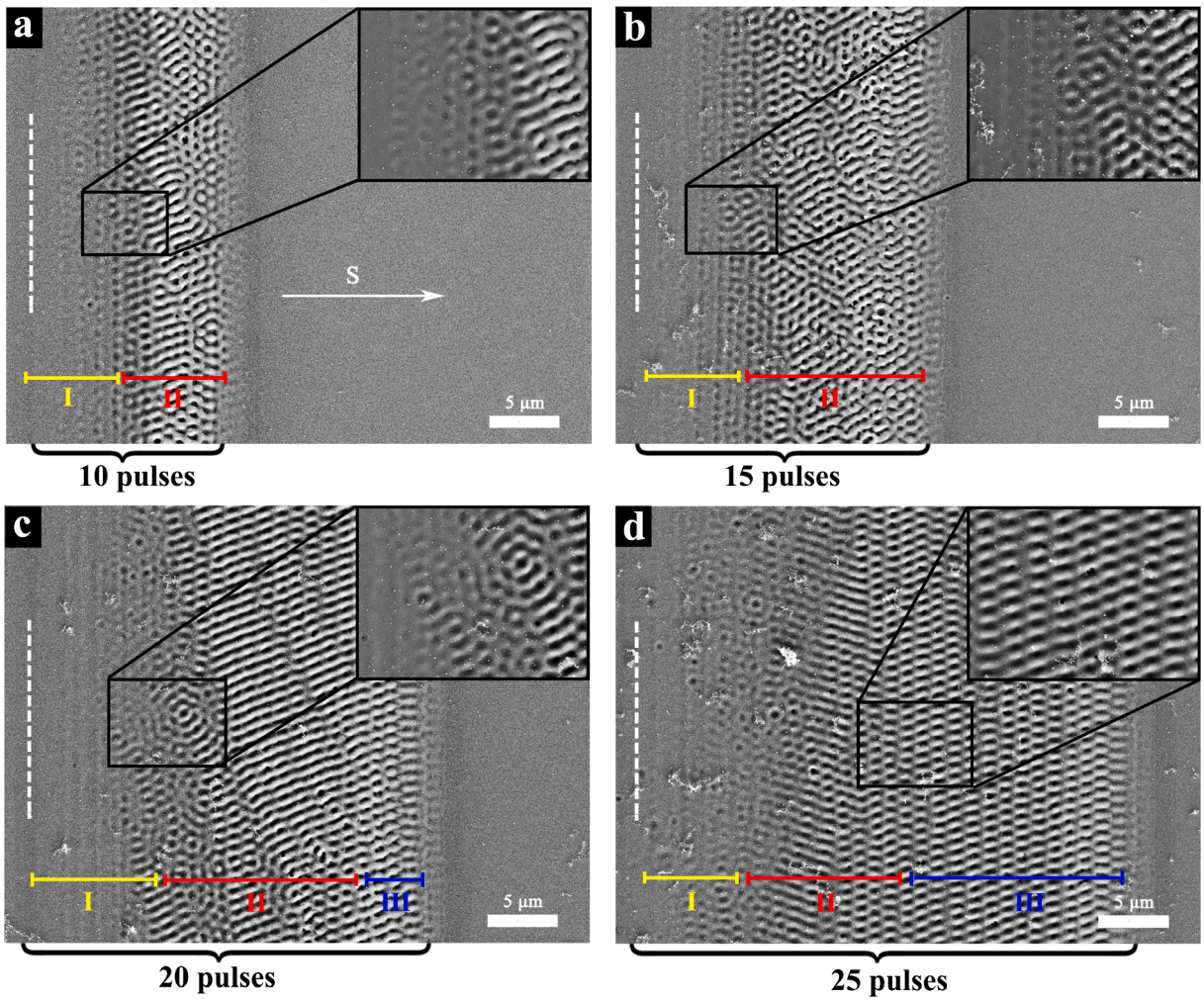

Fig. 3. (a)-(d) SEM images of the Si surface morphology irradiated by different laser pulse numbers of 10, 15, 20, 25. The white arrow indicates the direction of the scanning direction, and the white dotted lines for the position of the first laser pulse irradiation.

free electrons, and then followed by thermal melting, overheating of the liquid phase and rapid solidification into the amorphous phase [29,30]. In fact, after the femtosecond laser irradiation the single-crystalline silicon can be transformed into the polycrystalline or amorphous phases. In our case, as shown in Fig. 2b, the laser-induced 2D structure arrays with nanodots distribution appear to provide the rough surface, which might contain polycrystalline, amorphous and oxidation components [31,32]. In order to make the morphology appearance smooth, we employed the 5 % HF as an etching regent to eliminate the amorphous and oxide materials, because of their etching rate much larger than that of the crystal. A SEM image of the structure morphology after 45 min etching in HF is shown in Fig. 2e, where the sharp structure profile with less particle depositions are observed. The further AFM characterization, as shown in Fig. 2f, indicates that HF etching process can lead to an increase not only in smoothness but also in depth of the structure arrays. The measured variation of the structure depth with the etching time is shown in Fig. 2g, where the modified structure depth seems to firstly increase from 75 nm to the maximum of 112 nm under 45 min etching. More interestingly, as the etching time further increases, the variation of the structure depth was seen to have a decreasing tendency. As the previously mentioned, because the etching rate of HF for the amorphous silicon is faster than that for the crystalline silicon, the amorphous part can be gradually removed from the surface and even completely peeled off at the large etching time of about 45 min. After that, the crystalline silicon material begins to be etched by HF at the slow speed, leading to no increase of the structure depth any more, or even a slightly decreased depth. The evolution of the surface morphology with the etching time is shown in Fig. S4.

3.2. *Formation mechanisms of the 2D nanostructure arrays*

The formation mechanisms of the aforementioned periodic 2D nanostructure arrays can be attributed to the self-regulatory of SPP excitation. In order to understand this effect, we first investigated the dynamic evolution of the surface morphology by effective controlling the numbers of femtosecond laser pulse irradiation on the material surface via the electrical shutter, and at least 10 pulses are allowed to pass within the time of its opening. Fig. 3a-d show the observations after irradiating 10, 15, 20 and 25 laser pulses on the surface during the sample scanning, at the given scanning speed of V = 1.2 mm/s and the laser energy fluence of F = 245.65 mJ/cm^2. Obviously, the surface morphology is seen to vary with the increase of pulse numbers partially overlapped along the scanning direction.

Generally, the change of surface morphology can be divided into three parts: the initial damaged region (I), the disordered structure region (II) and the regular structure region (III). The region I is generated by at first striking of a few laser pulses to roughen the flat surface with the presence of the ablated parallel shallow grooves and the random nanoparticles, the former of which is in fact created by the cylindrical focusing line-shaped laser beam spot, with the adjacent spatial distance depending on the scanning speed. This is much different from the previous studies of the structure formation by the laser focusing of the

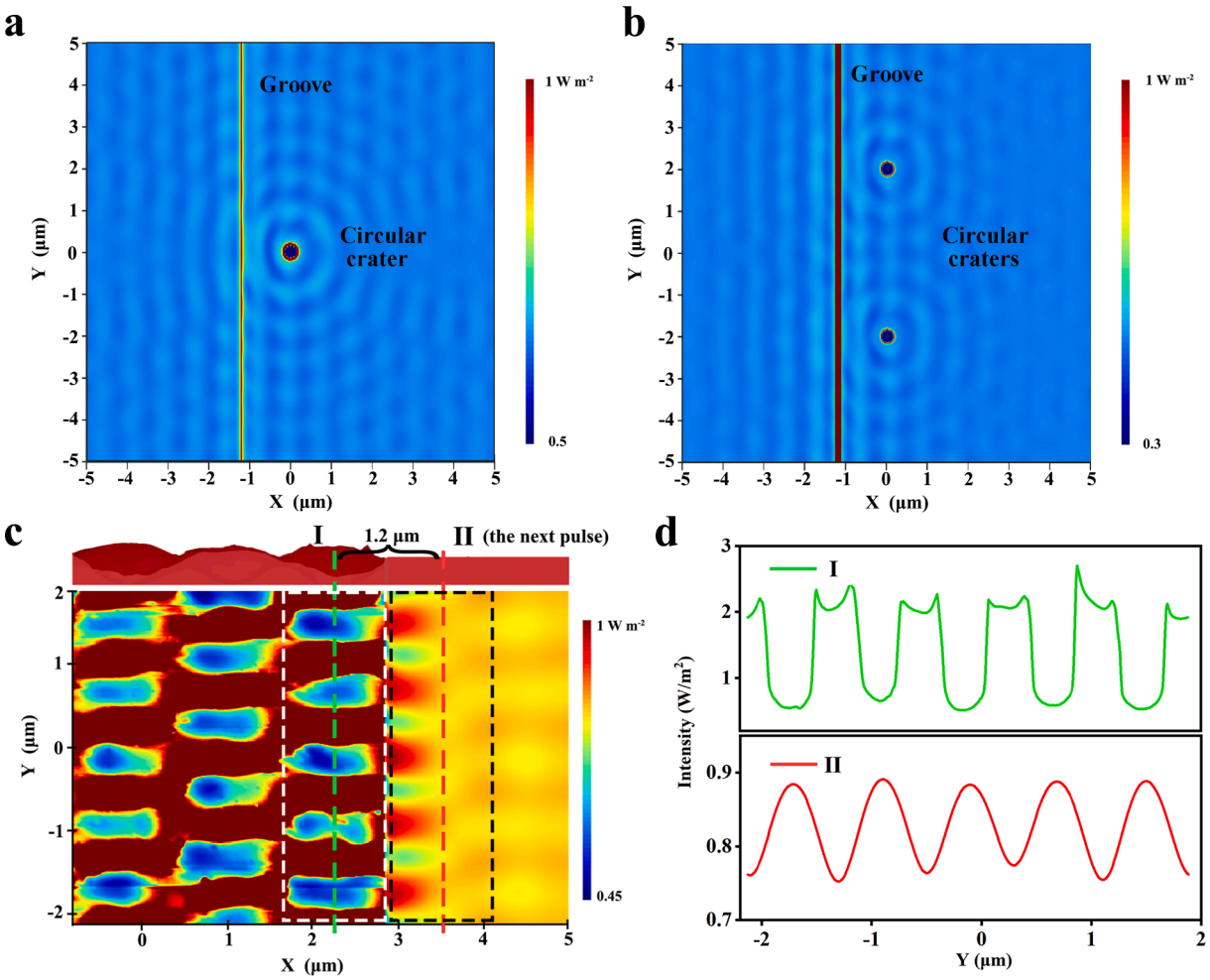

Fig. 4. FDTD simulation of the intensity distribution in different regions. (a)-(b) The disordered region. (c) The final regular region. (d) The E-field intensity in the center part of the last period (I) and the Si plane (II).

spherical lens, where a circular or elliptical profile is usually presented on the initially damaged surface region [25,26,28,33]. Noticeably, here the appearance of the shallow parallel ablation grooves is crucial for the subsequent formation of the 2D structure arrays. With increasing the number of laser pulses to N = 15 (Fig. 3b), the surface morphology appears to evolve into a disordered profile, associated with the groove splitting and the finer stripes formed inside. As the number of laser pulse irradiation reach N = 25 (Fig. 3d), the surface morphology turns into the uniform structure formation. In other words, the dynamic evolution of the surface morphology can be understood as follows: the initial laser pulses acting on the material often lead to the rough surfaces through the ablation behavior, which provides the basic conditions for the SPP excitation of the subsequent laser pulse irradiation [34,35]. On the rough surface consisting of nanoparticles, the light is diffracted into components with different wave vectors, which certainly provides the feasible coupling to satisfy the physical conditions of the SPP excitation on the interface. As a result, the laser intensity distribution will be modulated and the SPP excitation is affected by the ablation patterns, while the modulated energy in turn affects the change in the surface morphology. With the repeated mutual modulation between the surface morphology and the SPP excitation, the stable structure formation will be eventually achieved, which is the so-called self-regulatory process.

In order to better clarify the self-regulatory effect in the structure arrays formation, we put forward the FDTD simulations of the near-field distribution of the laser energy modulated by the structures via the SPP excitation (the model details are shown in Fig. S2 c). As shown in Fig. 4a-b, when the groove with one or two circular craters standing nearby was assumed for the modeling, the laser-SPP interference generated by these objects can be achieved on the material surface, leading to the spatial intensity distribution profiles similar to the patterns of the aforementioned disordered structure region II. In order to explore the modulated laser intensity distribution by the surface structure, we employed the AFM measured morphology of the structure arrays for the FDTD simulation, where the region I is the final arriving place of the previous laser pulses. And the region II is the smooth surface ready for the irradiation by the next laser pulse; moreover, the spacing between and regions I and II is set as 1.2 μm according to the scanning speed. It is seen clearly there are more laser energy localized inside the valley regions of the surface structure. Fig. 4(d) shows the SPP distributions of the two regions in Fig. 4(c), which confirms the near-field modulation effect of the existing surface structure on the subsequent irradiation of laser pulse. Meanwhile, the simulation result of Fig. 4 (d) confirms the simulated SPP distributions on two regions (I and II) seem to be regular but with spatial mismatching each other. Thus, when the next laser pulse arrives at the region II, the newly generated surface structures based on the laser-SPP interference is also regular but with the mismatched spatial arrangement in relevant to the structure in region I. In other words, once the regular structures are formed, its modulation on the subsequent laser irradiation tends to make the new structures develop in a regular way.

Furthermore, we employed a physical model developed by Hampp [24], to evaluate the dynamical evolution process of the surface morphology under irradiation of femtosecond laser pulses. First, the understanding of the physical properties for the SPP excitation around the sources is very critical for the dynamical evolution process. In order

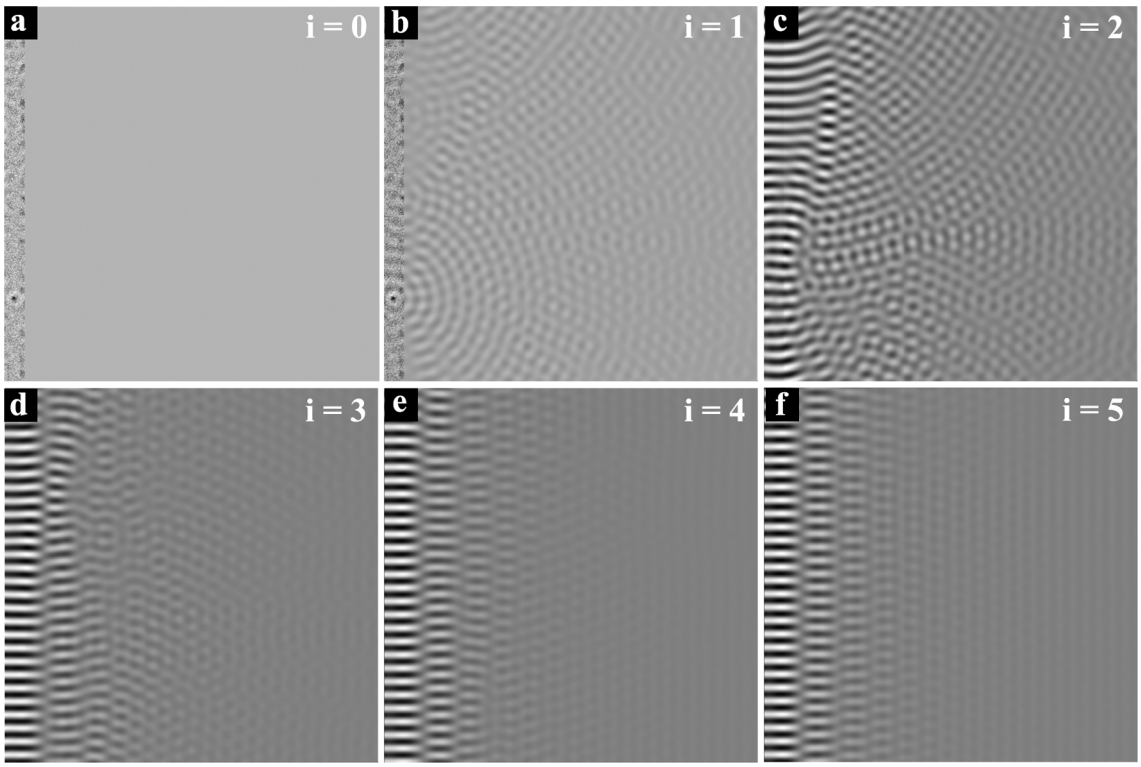

Fig. 5. Simulated interference patterns with different iterations by DIPF. (a) The imported SEM image for building up the initial SPP excitation source. (b-f) The results of the laser-SPP interference after 1 to 5 iterations.

to compare the SPP excitation behaviors by the circularly and linearly polarized lights, we calculated the E-field distribution around the nanoparticle with the FDTD method. As shown in Fig. S5, the SPP excitation has a uniform distribution in all directions for the incident circularly polarized light, while it only propagates along one direction under the linearly polarized light. As a matter of fact, such kind of laser polarization dependent SPP propagation can be also manifested by the obtained variable surface morphologies on the material surface (Fig. S6), in which the periodic 2D nanostructures can only be formed by the all-direction uniform distribution of SPP excitation under the circularly polarized light irradiation. Then, the feedback loop is based on the excitation sources through the SEM observation, and the laser-SPP interference patterns at the position of the following laser pulse irradiation is obtained by the iterative simulation process [17,36], and the details of calculation can be found in the supplement B.

In the simulation, we selected an area within the initially laser-damaged region to start the calculation (Fig. 5a).The simulation results after 1–5 iterations are shown in Fig. 5b-f, which are strikingly similar to the experimental observations and well illustrate three stages during the formation of surface structures. The results of the first and second iterations indicate that the laser-SPP interference is ready to transform the flat surface into the random patterns, which corresponds

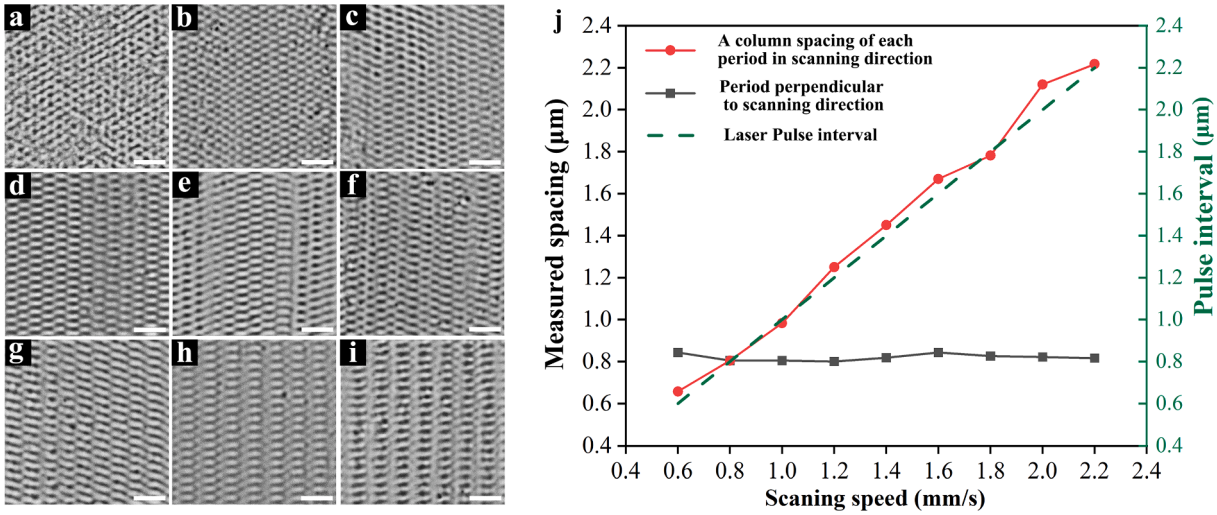

Fig. 6. (a-i) Morphology of 2D periodic nanostructure arrays with the laser scanning speeds of 0.6 mm/s, 0.8 mm/s, 1 mm/s, 1.2 mm/s, 1.4 mm/s, 1.6 mm/s, 1.8 mm/s, 2 mm/s and 2.2 mm/s, respectively. The scale bar in these figures are all 3 μm. (j) The corresponding measured spacing of the structure and pulse intervals with varying laser scanning speeds.

to the disordered structure region during the accumulated laser pulse irradiation experiment. As the iteration step increases, the simulated spatial distribution of the interference patterns tends to be regular (Fig. 5e and 5f). Because the obtaining DIPF result is based on the continuous modulation between the structure morphology and the surface wave excitation, it can well explain the self-regulatory effect during the regular structure formation. However, it should be mentioned that, the simulation of surface morphology reaches the regular distribution after 5 iterations, while the experimentally observed uniform structure arrays were achieved after 10 pulses irradiation. This may be due to the different nanoparticle distribution between them to affect the SPP excitation.

The patterns in Fig. 3 are the engraving results of different numbers of laser pulses at the same scanning speed, which indicate that the formation of the regular structure arrays requires a certain number of laser pulses accumulated on the material surface. The experimental results showed that the effect of each laser pulse irradiation on the material surface is spatially separated, associated with the particular surface morphology formation. In addition, the simulation result in Fig. 5 was actually based on the laser-SPP interference to present a dynamic evolution of surface wave self-regulatory process, which can reveal the positive feedback modulations between the surface morphology and SPP excitation during the laser processing. Thus, during the iterative processes of DIPF simulation, the influence of each pulse is considered in the dynamic evolution to show its own related interference pattern. In summary, the reason for the formation of regular structure is the interference between each laser pulse and the SPP of its location.

3.3. *Modulation of surface morphology for 2D nanostructure arrays*

Based on the above discussion, the mutual modulation between the surface morphology and the SPP excitation plays a key role in controlling the final structure formation. Because each column of the structure formation within 2D arrays is in fact generated by the laser pulse irradiation at this place, the spatial interval of the adjacent laser pulses will certainly affect the SPP distribution and morphology construction. To better understand this effect, we carried out the additional experiments by varying the scanning speed to control the pulse for the morphology change, and the corresponding SEM images of the results were displayed in Fig. 6a-i. With the increase of the scanning speed, the structure period in the direction perpendicular to the scanning direction is able to maintain while it gradually increases in the scanning direction. The measured statistical relationship between these parameters is plotted in Fig. 6j, which indicates the constant period of $\Lambda = 800$ nm along the direction perpendicular to the scanning direction and a column spacing of each period increase along the scanning direction in proportion to the scanning speed. In other words, because the spatial interval of the adjacent laser pulses arriving at the surface plays an important role in the self-regulatory process, it is possible to control the structure period by simply adjusting the scanning speed.

4. Conclusions

This study has deeply investigated a maskless effective method for one-step fabricating the regular arrangement of 2D periodic nanostructures on Si surface, using the cylindrical focusing of femtosecond laser pulses with circular polarization. The experimental results have demonstrated that the uniform structure arrays can be obtained with fine adjusting the scanning speed. The formation mechanisms are attributed to the self-regulatory effect of the SPP excitation from the modulation of the transient surface morphology, which is sufficiently confirmed by both the FDTD and DIPF simulations. It is believed that our deep insights for the 2D formation of nanostructure arrays will benefit the understanding of the femtosecond laser regular surface structuring and applications.

Funding

Natural Science Foundation of China (NSFC, Grant Nos. 91750205, 61705227), Jilin Provincial Science & Technology Development Project (Grant No. 20200201086JC), K. C. Wong Education Foundation (GJTD-2018-08), Opening Project of the Key Laboratory of Bionic Engineering (Ministry of Education), Jilin University, K201905.

Declaration of Competing Interest

The authors declare that they have no known competing financial interests or personal relationships that could have appeared to influence the work reported in this paper.

Data availability

Data will be made available on request.

Appendix A. Supplementary data

Supplementary data to this article can be found online at https://doi.org/10.1016/j.apsusc.2022.154615.

References

[1] Z. Dong, J. Ho, Y.F. Yu, Y.H. Fu, R. Paniagua-Dominguez, S. Wang, A.I. Kuznetsov, J.K.W. Yang, Printing beyond sRGB color gamut by mimicking silicon nanostructures in free-space, Nano Lett. 17 (2017) 7620–7628.
[2] M. Khorasaninejad, W.T. Chen, R.C. Devlin, J. Oh, A.Y. Zhu, F. Capasso, Metalenses at visible wavelengths: Diffraction-limited focusing and subwavelength resolution imaging, Science 352 (2016) 1190–1194.
[3] M.I. Shalaev, J. Sun, A. Tsukernik, A. Pandey, K. Nikolskiy, N.M. Litchinitser, High-efficiency all-dielectric metasurfaces for ultracompact beam manipulation in transmission mode, Nano Lett. 15 (2015) 6261–6266.
[4] Y. Yang, W. Wang, A. Boulesbaa, D.P. Kravchenko II, A. Briggs, D. Puretzky, J. V. Geohegan, Nonlinear fano-resonant dielectric metasurfaces, Nano Lett. 15 (2015) 7388–7393.
[5] R. Ahmed, A.K. Yetisen, S.H. Yun, H. Butt, Color-selective holographic retroreflector array for sensing applications, Light Sci. Appl. 6 (2017) e16214.
[6] W. Cao, L. Jiang, J. Hu, A. Wang, X. Li, Y. Lu, Optical field enhancement in au nanoparticle-decorated nanorod arrays prepared by femtosecond laser and their tunable surface-enhanced raman scattering applications, ACS Appl. Mater. Interfaces 10 (2018) 1297–1305.
[7] J. Huang, L. Jiang, X. Li, Q. Wei, Z. Wang, B. Li, L. Huang, A. Wang, Z. Wang, M. Li, L. Qu, Y. Lu, Cylindrically focused nonablative femtosecond laser processing of long-range uniform periodic surface structures with tunable diffraction efficiency, Adv. Opt. Mater. 7 (2019).
[8] S. Daqiqeh Rezaei, J. Ho, T. Wang, S. Ramakrishna, J.K.W. Yang, Direct color printing with an electron beam, Nano Lett. 20 (2020) 4422–4429.
[9] P. Shi, J. Zhang, H.-Y. Lin, P.W. Bohn, Effect of molecular adsorption on the electrical conductance of single Au nanowires fabricated by electron-beam lithography and focused ion beam etching, Small 6 (2010) 2598–2603.
[10] X.-F. Jia, L.-J. Wang, N. Zhuo, J.-C. Zhang, S.-Q. Zhai, J.-Q. Liu, S.-M. Liu, F.-Q. Liu, Z. Wang, Multi-wavelength sampled Bragg grating quantum cascade laser arrays, Photonics Res. 6 (2018) 721–725.
[11] K. Sugioka, Y. Cheng, Ultrafast lasers—reliable tools for advanced materials processing, Light Sci. Appl. 3 (2014) e149–e.
[12] A.Y. Vorobyev, C. Guo, Direct femtosecond laser surface nano/microstructuring and its applications, Laser Photonics Rev. 7 (2013) 385–407.
[13] L. Jiang, A.D. Wang, B. Li, T.H. Cui, Y.F. Lu, Electrons dynamics control by shaping femtosecond laser pulses in micro/nanofabrication: modeling, method, measurement and application, Light Sci. Appl. 7 (2018) 17134.
[14] J.F. Young, J.S. Preston, H.M. van Driel, J.E. Sipe, Laser-induced periodic surface structure. II. Experiments on Ge, Si, Al, and brass, Phys. Rev. B 27 (1983) 1155–1172.
[15] J.E. Sipe, J.F. Young, J.S. Preston, H.M. van Driel, Laser-induced periodic surface structure. I. theory, Phys. Rev. B 27 (1983) 1141–1154.
[16] D.C. Emmony, R.P. Howson, L.J. Willis, Laser mirror damage in germanium at 10.6 μm, Appl. Phys. Lett. 23 (1973) 598–600.
[17] W.L. Barnes, A. Dereux, T.W. Ebbesen, Surface plasmon subwavelength optics, Nature 424 (2003) 824–830.
[18] J. Huang, L. Jiang, X. Li, A. Wang, Z. Wang, Q. Wang, J. Hu, L. Qu, T. Cui, Y. Lu, Fabrication of highly homogeneous and controllable nanogratings on silicon via chemical etching-assisted femtosecond laser modification, Nanophotonics 8 (2019) 869–878.
[19] T. Zou, B. Zhao, W. Xin, Y. Wang, B. Wang, X. Zheng, H. Xie, Z. Zhang, J. Yang, C. L. Guo, High-speed femtosecond laser plasmonic lithography and reduction of graphene oxide for anisotropic photoresponse, Light Sci. Appl. 9 (2020) 69.

[20] M. Huang, F.L. Zhao, Y. Cheng, N.S. Xu, Z.Z. Xu, Origin of Laser-Induced Near-Subwavelength Ripples: Interference between Surface Plasmons and Incident Laser, Acs Nano 3 (2009) 4062–4070.
[21] E.V. Golosov, A.A. Ionin, Y.R. Kolobov, S.I. Kudryashov, A.E. Ligachev, Y. N. Novoselov, L.V. Seleznev, D.V. Sinitsyn, Ultrafast Changes in the Optical Properties of a Titanium Surface and Femtosecond Laser Writing of One-Dimensional Quasi-Periodic Nanogratings of Its Relief, J. Exp. Theor. Phys.+ 113 (2011) 14–26.
[22] X. Zheng, B. Zhao, J. Yang, Y. Lei, T. Zou, C. Guo, Noncollinear excitation of surface plasmons for triangular structure formation on Cr surfaces by femtosecond lasers, Appl. Surf. Sci. 507 (2020).
[23] S.A. Jalil, J. Yang, M. ElKabbash, C. Cong, C. Guo, Formation of controllable 1D and 2D periodic surface structures on cobalt by femtosecond double pulse laser irradiation, Appl. Phys. Lett. 115 (2019).
[24] S. Durbach, N. Hampp, Generation of 2D-arrays of anisotropically shaped nanoparticles by nanosecond laser-induced periodic surface patterning, Appl. Surf. Sci. 556 (2021).
[25] R. Goodarzi, F. Hajiesmaeilbaigi, Circular ripple formation on the silicon wafer surface after interaction with linearly polarized femtosecond laser pulses in air and water environments, Opt. Quant. Electron. 50 (2018).
[26] O. Varlamova, F. Costache, J. Reif, M. Bestehorn, Self-organized pattern formation upon femtosecond laser ablation by circularly polarized light, Appl. Surf. Sci. 252 (2006) 4702–4706.
[27] J.-T. Zhu, Y.-F. Shen, W. Li, X. Chen, G. Yin, D.-Y. Chen, L. Zhao, Effect of polarization on femtosecond laser pulses structuring silicon surface, Appl. Surf. Sci. 252 (2006) 2752–2756.
[28] O. Varlamova, F. Costache, M. Ratzke, J. Reif, Control parameters in pattern formation upon femtosecond laser ablation, Appl. Surf. Sci. 253 (2007) 7932–7936.
[29] S.K. Sundaram, E. Mazur, Inducing and probing non-thermal transitions in semiconductors using femtosecond laser pulses, Nat. Mater. 1 (2002) 217–224.
[30] M. Garcia-Lechuga, D. Puerto, Y. Fuentes-Edfuf, J. Solis, J. Siegel, Ultrafast Moving-Spot Microscopy: Birth and Growth of Laser-Induced Periodic Surface Structures, ACS Photonics 3 (2016) 1961–1967.
[31] M.O. Thompson, J.W. Mayer, A.G. Cullis, H.C. Webber, N.G. Chew, J.M. Poate, D. C. Jacobson, Silicon Melt, Regrowth, and Amorphization Velocities during Pulsed Laser Irradiation, Phys. Rev. Lett. 50 (1983) 896–899.
[32] R. Tsu, R.T. Hodgson, T.Y. Tan, J.E. Baglin, Order-Disorder Transition in Single-Crystal Silicon Induced by Pulsed Uv Laser Irradiation, Phys. Rev. Lett. 42 (1979) 1356–1358.
[33] R. Sugawara, S. Sekiguchi, T. Yagi, Formation of periodic ripples through excitation of ~1μm spot using femtosecond-laser Bessel beam on c-Si, Appl. Surf. Sci. 353 (2015) 400–404.
[34] J. Bonse, A. Rosenfeld, J. Krüger, On the role of surface plasmon polaritons in the formation of laser-induced periodic surface structures upon irradiation of silicon by femtosecond-laser pulses, J. Appl. Phys. 106 (2009).
[35] A.V. Zayats, I.I. Smolyaninov, Near-field photonics: surface plasmon polaritons and localized surface plasmons, J. Opt. a-Pure Appl. Op. 5 (2003) S16–S50.
[36] K. Sokolowski-Tinten, D. von der Linde, Generation of dense electron-hole plasmas in silicon, Phys. Rev. B 61 (2000) 2643–2650.